Proceedings of the 17th World Congress
The International Federation of Automatic Control
Seoul, Korea, July 6-11, 2008

Wireless Distributed Architecture for Therapeutic FES: Metrology for muscle control

M. Toussaint, Jr. [*] **D. Andreu** [**] **P. Fraisse** [*,**]

[*] *LIRMM-CNRS, University of Montpellier 2, France (e-mail: philippe.fraisse@lirmm.fr, mickael.toussaint@lirmm.fr).*
[**] *INRIA, Sophia Antipolis, France (e-mail: david.andreu@inria.fr)*

Abstract: This paper presents a Functional Electro-Stimulation distributed architecture based on a wireless network, for therapeutic training of disabled patients. On this distributed architecture, the movement (of disabled members) is artificially controlled by means of a global controller which pilots a set of stimulation units. The closed loop control system we developed for controlling muscle is based on a high order sliding mode method. In such wireless network-based control, the variable delay introduced by the network must be taken into account to ensure the stability of the closed loop. Thus, in order to characterize the medium on which the control is performed, we carried out accurate measurements of the architecture performances (stack-crossing, round-trip time, etc.). We then propose the use of a Kalman filter to predict the communication delay evolution, with the aim to exploit it within the closed loop control.

1. INTRODUCTION

Electrical stimulation can generate an artificial contraction of skeletal muscles by applying sequences of electrical pulses to sensory-motor system via electrodes which can be placed on the skin, [Kralj et al., 1980], or implanted [Guiraud et al., 2006]. Transcutaneous (surface) electrical stimulation is a technique widely applied for physical therapy, sports training and clinical purposes. It can be used for muscle atrophy treatment, muscle force training, endurance training, pain treatment and functional movement therapy [Keller et al., 2006]. Functional Electrical Stimulation (FES) concerns the restoration of a functional movement in disabled patients. FES applications applied to lower limbs include foot drop correction, single joint control, cycling, standing up, walking... FES applications applied to upper limbs allow hand grasping enhancement. A wide range of disabilities are concerned with FES, they include spinal cord injuries, stroke, multiple sclerosis; cerebral palsy and Parkinson's disease [Prodanov et al., 2003] and both children and adults are concerned. Two distinct objectives may be targeted when using those techniques, depending on the type of disorder: chronic assistance or acute training. FES can be applied for example for walking assistance and training in post-stroke hemiplegic patients, as well as for standing and gait restoration in paraplegic patients [Heliot et al., 2007]. Physiological effects of FES-assisted verticalization in paraplegic patients include for example: prevention of muscle atrophy, promotion of renal functions, improvement of joint range of motion, well being, improved digestion, bowel and bladder functions, retardation of bone-density loss, decreased spasticity, reduced risks of pressure sores, improved cardiovascular health, improved skin and muscle tone [Cybulski and Jaegger, 1986]. The FES used in the framework of exercise was termed Functional Electrical Therapy (FET).

In this context of FET, stimulators which are used are wire-based and centralized ones; each electrode is connected to a central controller by means of wires (the number of wires for each electrode depending on its number of poles). Those electrodes being used for stimulation or recording (external sensors based on EMG for example), of the sensory-motor system activity. When dealing with a set of (multipolar) electrodes, those wires constitute an important constraint for the patient mobility, and thus for the training. This constraint must be removed to propose realistic solutions for rehabilitation applications to be used by physiotherapist and/or the patient himself. As a consequence we designed a distributed FES architecture based on distributed stimulation units (DSU) [Andreu et al., 2005].

Each DSU is a device composed of digital and analogue parts, the latter being connected to the (multipolar) electrode used to stimulate the muscle. A DSU can be configured, programmed and remotely operated [Souquet et al., 2007]. It embeds in particular a 3-layer protocol stack according to the reference given by the structure of the reduced OSI model. These layers are the Application layer, the Medium Access Control layer (MAC) and the Physical layer. The physical layer ensures the telecommunication over the 2.4 GHz Radio Frequency (RF) based wireless medium (used in considered experimental setup). The MAC layer ensures a deterministic medium sharing [Godary et al., 2007]. The application layer supports configuration, programming and remote operating (from start/stop requests to online stimulation control) of the stimulation unit.

On this distributed architecture, the movement (of disabled members) is artificially controlled by means of a global controller which pilots a set of DSUs. For instance, it sets dynamically the parameters of the stimulation, like the stimulation frequency, the pulse amplitude and

width. It selects and remotely controls the subset of DSU implied in the current phase of the movement (the MAC protocol allowing multicast exchanges). The closed loop control system we use for muscle control is based on a high order sliding mode controller: we applied it to the FES-based control of the knee joint by co-contraction of quadriceps and hamstring muscles [Mohammed et al., 2005]. But in case of (wireless) network-based control, the variable delay introduced by the network must be taken into account to ensure the stability of the closed loop [Fraisse and Leleve, 2003], [Turchi et al., 1997]. If the delay is bounded and its variation is predictable, there exists a stable controller. Thus, in order to characterize the medium on which the control will be performed, we carried out precise measurements of the architecture performances (stack-crossing, round-trip time, etc.).

The paper begins with a brief state of the art in the context of FES-based muscle control, presented in section 2 to highlight control issues in this context. Section 3 exposes the experimental setup which has been used for the metrology, principle and results of which are then given section 4. For network-based muscle control, a predictive filter is then studied in section 5.

2. MUSCLE CONTROL

Although, open loop control strategy does not account for any changes in the muscles performance such as fatigue or load changes, they have been widely used in clinics due to their relative simple implantation [Bajd et al., 1981]. Closed loop system as reported in many studies, uses sensor feedback to update the stimulation level (intensity and pulse width) as a response to any extern disturbances. Some authors used a simple PID controller [Wood et al., 1998], Knee Extension Controller KEC [Poboroniuc et al., 2003], a combination of feedback and feedforward control. Others used a first or a second order switching curve in the state space to control patients movements: the On/Off controller [Mulder et al., 1992], in the so-called "controller-centered". The main advantage of these strategies is their low number of parameters to be tuned during stimulation. The so-called "subject-centered" strategies introduce the voluntary contribution of the upper body of the patient as an essential part of the control diagram: PDMR [Riener and Fuhr, 1998], CHRELMS [Donaldson and Yu, 1996]. This latter still is far to be adopted because of the relative high number of parameters to be identified.

In order to overcome for the mentioned drawbacks, a better understanding of the muscle element as well as finding a compromise between a complex control strategy and a satisfactory one, should be taken into account. To accomplish this task, we use a new mathematical based muscle model (Fig. 1), described in previous studies, representing the most complex physiological process [El Makssoud et al., 2003].

The recruited motor units increase as a function of both intensity stimulation I and pulse width PW. This is modeled by 2 models. The activation model represents the ratio of recruited fibres with the generated chemical substance which control the muscle contraction. The mechanical model gives the force resulting from the muscle contraction and the muscle length returned by the biomechanical

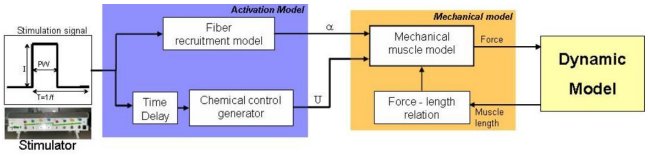

Fig. 1. The muscle model followed by the biomechanical model

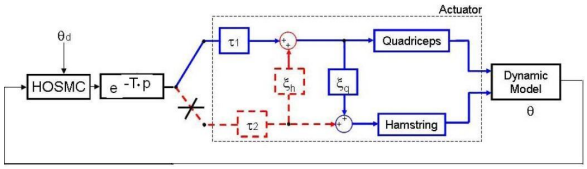

Fig. 2. Network delay introduced into control of muscles

model. The biomechanical model represents the knee joint acted by the muscle. The nonlinearities of the muscle model and the required robustness regarding parameters variations and external disturbances lead us to adopt a controller relying on the sliding mode theory. We developed a high order sliding mode controller (HOSM) and applied it to the control of the movement of the human knee under FES (Fig. 2).

However, controlling muscles stimulation over a network, a wireless one in our case, imposes to take into account in our control of muscles the variable delay introduced by the network (Fig. 2). We consider in this analyze both average and standard deviation of the delay, in order to manage and ensure the stability of the closed loop. To reach this objective, our approach is to dynamically adapt controller's parameters (gains) according to the delay. This obviously requires first to estimate and predict the delay and its variation.

Muscle co-contraction can be defined as the simultaneous activation of agonist and antagonist muscle groups crossing the same joint and acting in the same plane. The opposite muscles, quadriceps and hamstrings in this case, act simultaneously and thereby may increase the stiffness at the knee joint. The co-contraction phenomenon was represented by a simultaneous contraction of the muscle and its antagonist muscle via a static factor weighting ξq, ξh for quadriceps and hamstrings respectively. The amount of co-contraction was evaluated, based on a static linear constraints optimization of the muscle forces acting on the knee.

A method has been proposed [Mohammed et al., 2005] to define the contribution of the control vector u stemming from the 2-sliding controller to calculate the needed electrical current stimulation values. According to the sign of the resulting control variable u at the output of the HOSM controller and the value of ξi, we have chosen to stimulate whether the quadriceps, the hamstrings or both.

3. EXPERIMENTAL SETUP

For this experimental setup, the wireless distributed architecture is composed of the controller and 2 DSUs. Each DSU (Fig. 3) is prototyped on an *Altera Stratix development board*. This Stratix development board includes a Stratix FPGA with a *NiosII* soft-core embed-

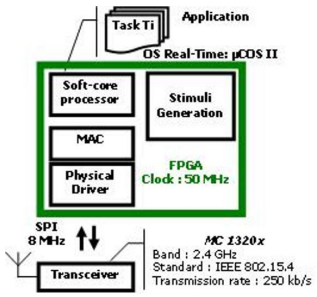

Fig. 3. Simplified description of the DSU architecture

ded processor. As medium, we use $MC1320x$ transceivers from *Freescale Semicondutor*, which are short range, low power, 2.4 GHz Industrial, Scientific, and Medical (ISM) band transceivers designed for the IEEE 802.15.4 standard wireless medium. The raw transmission rate is 250 kb/s.

The MC1320x transceiver is driven through the Serial Peripheral Interface (SPI). It is configured in half duplex and packet mode (received data is buffered in on-chip RAM). It stays in default reception mode to wait a frame. To emit a frame it has to be reconfigured in transmission mode.

A "physical driver" is implanted on the FPGA to ensure the interface between the upper layers of the protocol stack (which are medium-independent) and the MC1320x transceiver. It provides functions to control the transceiver. We use a Master/Slave MAC Protocol described in a hardware description language (HDL). This protocol STIMAP (patented) has been presented in [Godary et al., 2007]. Also implanted on the FPGA, It allows multicast, ensures deterministic group medium access management with sliding time interval, and filters received frames according to their destination logical address and manages the medium access.

Application layer, implemented as processes executed on the Nios II soft-core using $\mu COSII$ Real-Time Operating System, extracts data from incoming frames and launches desired actions. In these experiments, actions are mainly limited to management, configuration, metrology, and data storage on the entity.

Controller and DSUs use the same protocol stack, they rely on the same technology but they are different as they do not ensure the same functionalities. The controller executes the control law whereas each DSU embeds a stimulus generator (Fig. 3). Note that in experiments we present, the action executed by a DSU is limited to communication aspects (return of responses to the controller).

4. METROLOGY

4.1 Principles

The aim of this method is to characterize the wireless communication terms of transmission delay. The collected datas are reported to the application layer when an interruption signal occurs from a measure point and stored in real time. Measure points (MPt) are points where data (frame load) or events (frame reception) are reported to application layer (Fig. 4, Fig. 5). With the timer available

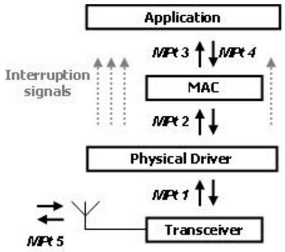

Fig. 4. Measure points

on the Nios II soft-core, data exchanged between application, MAC, and physical layers can be time-stamped in order to calculate stack-crossing times as well as Round-Trip Times (RTT between the controller and the DSU). When a frame is received, the number of received bytes and the Link Quality Indicator (LQI), which is a measure of the received signal level, are available into transceiver registers and can also be reported to the application layer.

When a frame is received by the transceiver, data is buffered in its on-chip memory and IT_pkt_rcv interruption signal (MPt 1) is asserted by the physical driver. If the Cyclic Redundancy Check (CRC) of the received frame is valid, the received frame, its number of bytes and the LQI are transmitted to the MAC layer. At this time the IT_MAC (MPt 2) is asserted and the application layer increments its counter of received frame and stores the number of bytes as well as the LQI. If the destination logical address of the frame is valid (i.e. if the DSU is concerned), data is sent to the application layer; IT_Mess (MPt 3) is then asserted. If the sender (i.e. the controller) required an acknowledgement, then the frame is returned to its sender (MPt 4). When the frame has been completely transmitted by the transceiver, the physical driver asserts the IT_pkt_snt (MPt 5).

4.2 Estimation

Both MAC and physical driver layers, are implemented on programmable logic, so we estimate time to go through MAC and Driver layers by functional simulation using Altera design software (for a 50 MHz clock frequency). Besides, frame transmission time, i.e. transmission of the frame bytes by the RF transceiver, and configuration time in transmission mode is given in the MC1320x reference manual. So we can determine the data processing time by the transceiver and our hardware described on the programmable logic. For all equations, data processing time is function of the frame size expressed in number of bytes N. Accessing to the transceiver on-chip memory takes 1.3 s per byte.

In case of reception, reception mode configuration takes 148 s. The time so that the physical driver asserts a frame reception is 10 s. Then, if the received frame is good (CRC is valid), the physical driver recovers the stored frame in the transceiver on-chip memory. Frame recovery time (FRT) is:

$$FRT = 10 + N \times 1.3 \quad (\mu s) \tag{1}$$

In case of transmission the transceiver introduces a latency of 400 s before starting a transmission Transmission mode

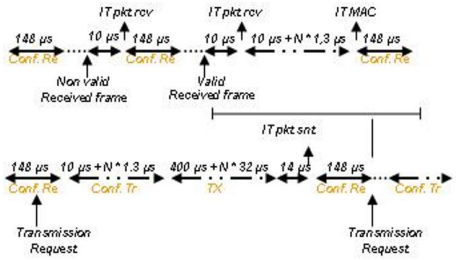

Fig. 5. Layer-crossing performances (reception and transmission)

configuration time (TMCT) and time of complete frame transmission (FTT) on the medium by transceiver are given by:

$$TMCT = 10 + N \times 1.3 \quad (\mu s) \tag{2}$$

$$FTT = 400 + N \times 32 \quad (\mu s) \tag{3}$$

After the transmission by the transceiver, time to assert the corresponding interruption is 14 μs. In some cases, the latency may vary. The transceiver can receive non valid frames coming from other protocols using 2.4 GHz band such as WiFi or Bluetooth; they are filtered due to an invalid CRC. We consider these frames as disturbances. When a non-valid frame is received, the transceiver has to be reconfigured, after frame reception assertion (10 μs), in reception mode before receiving a new frame. During this reconfiguration time (148 μs) no frame can be received. If a transmission request occurs during this reconfiguration in reception mode, the maximal latency before actual transmission will thus be of 148 μs plus TMCT for the configuration in transmission mode. As the physical driver is describe, the transceiver is always configured in reception mode before being configured in transmission mode. In this case if a transmission request occurs during a valid frame reception, the maximal latency, without TMCT, is:

$$FRML = 168 + N \times 1.3 \quad (\mu s) \tag{4}$$

Processing time by the MAC layer is estimated by simulation (50 MHz clock frequency). Reception (MRT) and transmission (MTT) times are respectively given by (5) and (6):

$$MRT = 1 + N \times 0.2 \quad (\mu s) \tag{5}$$

$$MTT = 0.6 + N \times 0.3 \quad (\mu s) \tag{6}$$

4.3 Measures

In this experiment 10 bytes frames are sent periodically by the controller to the 2 DSUs alternately and 14 bytes frames are returned in response by each DSU. Events at the MPts are reported to the DSU's application layer and time-stamped. and time to cross DSU's protocol-stack is measured (Fig. 6). It includes (cf. Table 1): the time to get the frame received by the physical layer, the MAC-layer crossing time, the application-layer treatment time and the whole protocol-stack crossing for transmission of the response. Fluctuations that can be observed on Fig. 6 are mainly due to the application-layer treatment time: this treatment on the embedded NIOS varies from 307 μs to 338 μs.

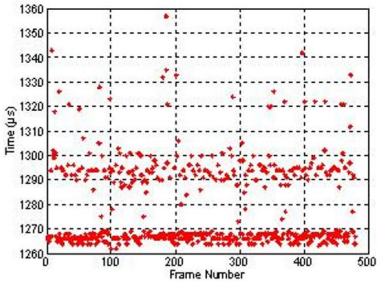

Fig. 6. Time to cross DSU's protocol-stack (for 10 bytes frames, in reception)

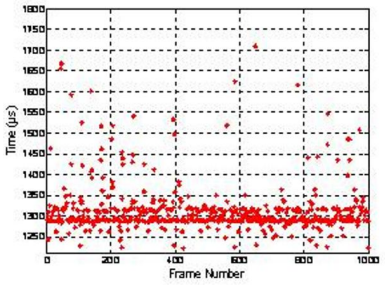

Fig. 7. RTT measured at the physical layer (controller side)

Table 1: Prediction vs Maximum Measure

Layers-crossing	Prediction	Measure
Phys. Driver in Reception	23 μs	27 μs
MAC in Reception	3 μs	4 μs
Layers-crossing Time in Rec.	**26** μs	**31** μs
Application	-	**338** μs
MAC in Transmission	5 μs	-
Phys. Driver in Transmission	28 μs	-
Transceiver in Transmission	862 μs	-
Layers-crossing Time in Tr.	**895** μs	**926** μs
Layers-crossing Total Time	-	**1295** μs

Table 1 presents maximum measured vs. predicted values of layers-crossing time, for a 10 bytes received frame.

For a 10 bytes frame, RTT between the controller and a DSU at physical and application levels are measured (on the controller side) and given respectively Fig. 7 and Fig. 8. Time to cross the DSU communication-stack is 1295 μs. The RTT at controller physical level of the controller, i.e. the difference of time between the effective frame transmission and the reception of the response frame (i.e. it does not includes communication-stack crossing on the controller side), is 1320 μs. The measurements are in good agreement with the theoretical evaluation.

Transmission energy of each entity is 1 mW and measured reception energy, in other word LQI value, is expressed in dBm. Experiments are realized with both DSUs. A first test showed the reception energy is independent from the frame size. However it is observed 2 distinct reception signal levels according to each DSU: this difference is mainly due to the positioning of the DSU cards (relative positioning between the cards as well as their positioning in the environment, reflection of the wall for instance). In order to assess the influence of DSU and human proximity (medical context), we disturb the data transmission by

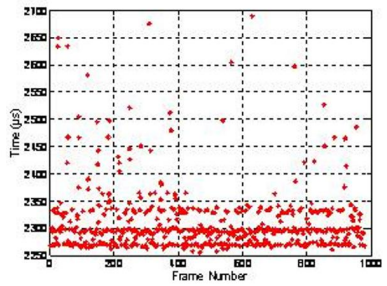

Fig. 8. RTT between controller and both DSUs, measured at the application layer (on the controller side)

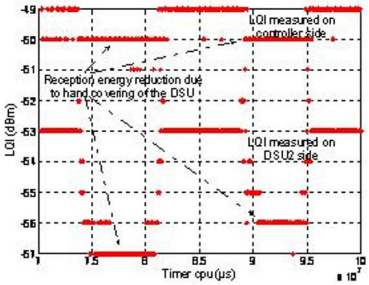

Fig. 9. LQI value, at controller and DSU sides, with and without hand covering of the DSU

covering the DSU with a hand. As a result a LQI value reduction is observed (Fig. 9). We can notice the impact on both sides: the LQI value is smaller, i.e. the signal is reduced, on the controller as well as on the DSU. Nevertheless, even in such situation the communication is not disabled.

In order to estimate the frame lost rate, frames have been exchanged, and stored in embedded memory to identify which have been lost, every 50 ms between the controller and a DSU, during 10 mn (hence 12000 frames exchanged depending on the memory capacity). The measured frame lost rate is 0.1 %. Note that the MAC layer does not ensure automatic retransmission of unacknowledged frames as we want to keep the entire control of the medium traffic; control over the network and control of the network are both considered. Unacknowledged frames, due to other wireless networks or noise on RF signal, are detected considering the theoretical RTT for an exchanged frame.

The radio environment of these experiments has not been modelled. However, there were in the vicinity of the experimental setup several IEEE 802.11b (WIFI)Access Points disturbing most probably the measurements presented previously. We can consider that the transceiver performs some algorithms to determine symbols and packets, detects the data, and filters pollution. No other system based on our protocol was present in the experimental environment so we measure no failure elimination at MAC level.

5. DELAY ESTIMATION FOR MUSCLE CONTROL

5.1 Objectives

In order to integrate communication delays within the control loop, these delays must be online measured and

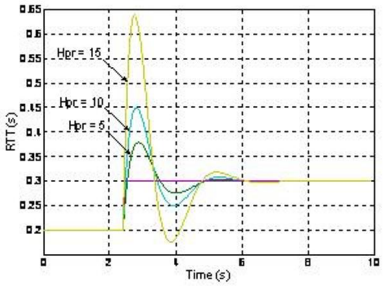

Fig. 10. Influence of the prediction horizon Hpr on the filter response (RTT prediction)

predicted. The aim is effectively to predict the evolution of the delay to adapt control law parameters. A discrete predictive Kalman filter associated with a double integrator model is used [Janabi-Sharifi et al., 2000] Matrices corresponding to this double integrator based model are given by (7). Kalman filter terms are given by (8). A is the transition matrix, Te is the sample rate (corresponding to frames transmission period), Q is covariance matrix, σ^2 is the covariance corresponding to measurement accuracy.

$$A = \begin{pmatrix} 1 & Te \\ 0 & 1 \end{pmatrix}; B = (0); C = (\,1\ 0\,) \tag{7}$$

$$R = \sigma^2; Q = \begin{pmatrix} 0 & 0 \\ 0 & \sigma^2 \end{pmatrix}; P_0 = I_2 \cdot \sigma^2 \tag{8}$$

Using double integrator model, noise is considered like the second derivate, in other word the delay acceleration. Kalman filter gives term of the delay estimation $\hat{X}_k$ and estimation on the prediction time horizon (Hpr) is given by (9).

$$\hat{X}_{k+Hpr} = A^{Hpr} \cdot \hat{X}_k \tag{9}$$

In case of packets losses, the strategy depends on the stimulation supervisory controller. In case of connection loss (not detected from a protocol point of view as we are not on a connected mode like that of Transmission Control Protocol TCP), the DSU automatically stops the stimulation if it did not receive any contol packet since a given time (timeout).

5.2 Characterization of the Kalman Filter

The Kalman filter is characterized by its step response according to parameters Te and Hpr, as they impact both the overshot and the response time. Fig. 10 shows the influence of the prediction time-horizon on the filter response, for Te being set to 50 ms.

5.3 Simulation

A prediction of mean RTT sinusoidal evolution is performed, by simulation, with a discrete predictive Kalman filter. The communication that is simulated is an exchange of frames every 5 ms during 10 s, and the prediction horizon is 100 ms. Parameters values are given in (10). Simulated RTT and predicted RTT present a similar evolution (Fig. 11), showing that the Kalman filter gives a good-enough prediction despite the 10 % overshot at the time of the discontinuity occurrence.

$$Te = 5ms; Hpr = 20; \sigma = 1\mu s \tag{10}$$

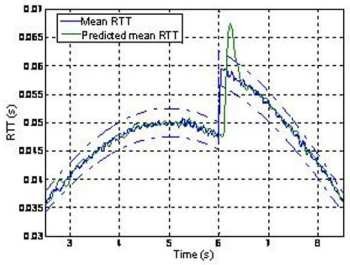

Fig. 11. Predicted vs. Simulated RTT

6. CONCLUSION

In this paper, we presented and analyzed in term of performance, a wireless distributed architecture for FES. We carried out experiments for estimating the delay and its variation according to frame payloads and disturbances in order to perform network-based closed-loop control on this architecture. We collected data from the experimental setup enabling a first estimation of communication performances (stack-crossing and RTT) between entities of this distributed architecture. Under these experimental conditions, both stack-crossing time and RTT are relatively constant, with a frame lost rate very low even in case of low reception signal level. The Kalman filter based real-time estimation of communication performances has shown that the prediction of the delay can be relevant. From those results on communication performance measurements and prediction, we currently adapt the HOSM control law in order to carry out the control of the movement of the human knee under wireless based distributed FES architecture. Our approach, which aims at guaranteeing the system stability under some limits, relies on a dynamical adaptation of the muscles control law parameters according to both measurement and prediction of communication delays. We will soon experiment this controller on the simulator we have developed (Fig. 1).

REFERENCES

Andreu, D. Techer, JD. Gil, T. and Guiraud, D. (2005) Implantable Autonomous Stimulation Unit for FES. 10th Annual Conference of the International Functional Electrical Stimulation (IFES'05), Montreal, Canada, July.

Bajd, T. Kralj, A. et al. (1981) Use of a two-channel functionnal electrical stimulator to stand paraplegics. Physical therapy, vol. 61, pp. 526-527.

Cybulski, G.R. and Jaegger, R.J. (1986) Standing Performance of Persons with Paraplegia. Arch. Phys. Med. Rehabil. vol. 67, pp. 103-108.

Donaldson, N. and Yu, C. (1996) FES standing control by handle reactions of leg muscle stimulation (CHRELMS). IEEE Transactions on rehabilitation engineering, vol. 4, pp.280-284.

Guiraud D, Poignet P., Wieber P. B., El Makssoud H., Pierrot F., Brogliato B., Fraisse P., Dombre E, Divoux J.C., Rabischong P., Modelling of the Human Paralysed Lower Limb Under FES, IEEE International Conference on Robotics and Automation 2003, pp. 2218-2223.

Fraisse, P. and Leleve, A. (2003) Teleoperation over IP Network : Network Delay Regulation and Adaptive Control. Journal of Autonomous Robots special Issue Internet Online Robots, Kluwer Academics Publishers, vol. 15, no. 3, pp. 225-235.

Godary, K. Andreu, D. and Souquet, G. (2007) Sliding Time Interval based MAC Protocol and its temporal validation. 7th IFAC International Conference on Fieldbuses and nETworks in industrial and embedded systems (FET'07), Toulouse, France, November.

Guiraud, D. Stieglitz, T. Koch, K.P. Divoux, J.L. and Rabischong, P. (2006) An implantable neuroprostheses for standing and walking in paraplegia: 5-year patient follow-up. Journal of Neural Eng., vol. 3, pp. 268-275.

Héliot, R. Azevedo, C. and Espiau, B. (2007) Functional Rehabilitation: Coordination of Artificial and Natural Controllers. In: Advanced Robotic Systems, Rehabilitation Robotics, pp. 164-186.

Janabi-Sharifi, F. Hayward, V. and Jason Chen, C. (2000) Novel adaptative discrete-time velocity estimation techniques and control enhancement of haptic interfaces. IEEE Transactions on Control Systems Techniology, vol. 6, no. 8, pp.1003-1009.

Keller, T. Kuhn, A. and Lawrence, M. (2006). Transcutaneous stimulation technology. Journal of Biomechanics, vol. 39.

Kralj, A. Bajd, T. and Turk, R. (1980) Electrical stimulation providing functional use of paraplegic patient muscles. Med Prog.Technol., vol. 7, pp. 3-9.

Mohammed, S. Fraisse, P. Guiraud, D. Poignet, P. and El Makssoud, H. (2005) Towards a Co-Contraction Muscle Control Strategy, IEEE Conference on Decision and Control, CDC'05, Seville, Spain, December.

Mulder, A. Veltink, P. and Boom, H. (1992) On/off control in FES-induced standing up: a model study and experiments. Med. and Biol. Eng. and Comput., vol. 30, pp. 205-212.

Poboroniuc, M. Wood, D. Donaldson, N. Fuhr, T.and Riener, R. (2003) Closed-loop control for FES-based restoration of standing in paraplegia. In: ISPRM.

Prodanov, D. Marani, E. and Holsheimer, J. (2003). Functional Electric Stimulation for sensory and motor functions: Progress and Problems. Biomedical Reviews, vol. 14, pp. 23-50.

Riener, R. and Fuhr, T. (1998) Patient-Driven Control of FES-Supported standing Up: A simulation study. IEEE Transactions on rehabilitation engineering, vol. 6, no. 2, pp.113-123.

Souquet, G. Andreu, D. and Guiraud, D. (2007) Intrabody network for advanced and efficient functional electrical stimulation. 9th International Workshop on Functional Electrial Stimulation, Vienna, Austria, September.

Turchi, H. Crosnier, A. and Fraisse, P. (1997) Real-time environment for mission programming of telerobotics systems, Telemanipulator and Telepresence, Technologies IV, SPIE: The International Society for Optical Engineering, Pittsburgh, Pennsylvania, October 14-15, 1997, pp. 22-29.

Wood, D. Harper, V. et al. (1998) Experience in Using Knee angles as part of a closed-Loop Algorithm to control FES-Assisted Paraplegic Standing. 6th Vienna International Workshop on Functional Electrical Stimulation, pp. 137-140.